Angular analysis of the $e^+e^- \to D^{(*)+}D^{*-}$ process near the open-charm threshold using initial state radiation at Belle

V. Zhukova
Belle Collaboration

"ALPS 2019", Obergurgl, 22-27 April 2019

Spectrum of charmonium

- Vector states above open-charm threshold are not fully understood
- Parameters of ψ states obtained from $\sigma_{\text{tot}}(e^+e^- \to \text{hadrons})$
  - are model-dependent
  - have large uncertainties
- Data collected should allow for coupled-channel analysis

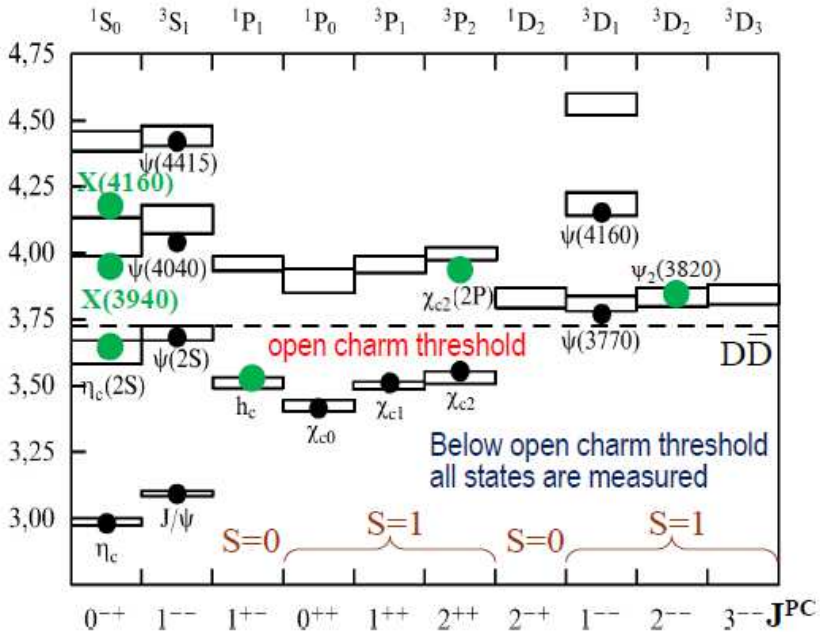

Spectrum of charmonium

- Vector states above open-charm threshold are not fully understood
- Parameters of ψ states obtained from $\sigma_{\text{tot}}(e^+e^- \to \text{hadrons})$
  - are model-dependent
  - have large uncertainties
- Data collected should allow for coupled-channel analysis

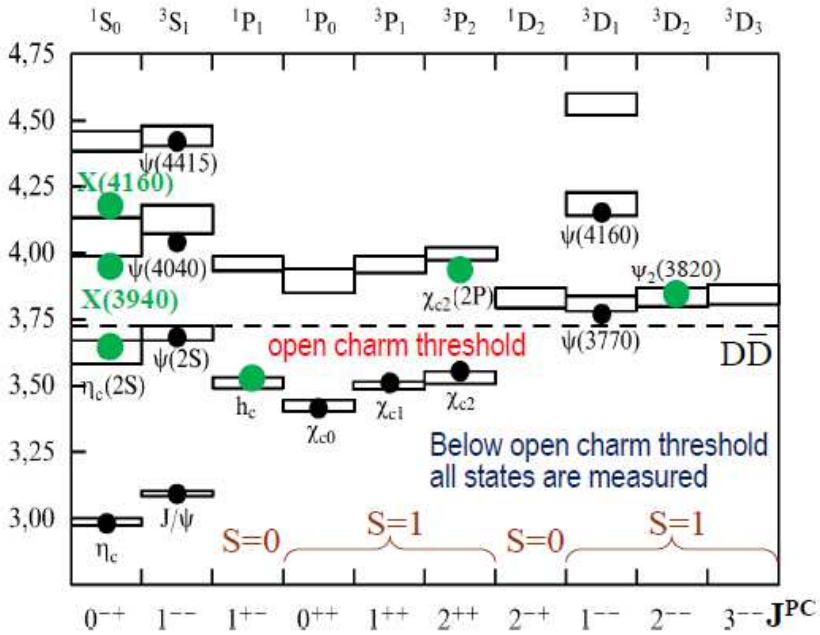

Solution $\Longrightarrow$ Measure exclusive cross sections

Comparison with previous results

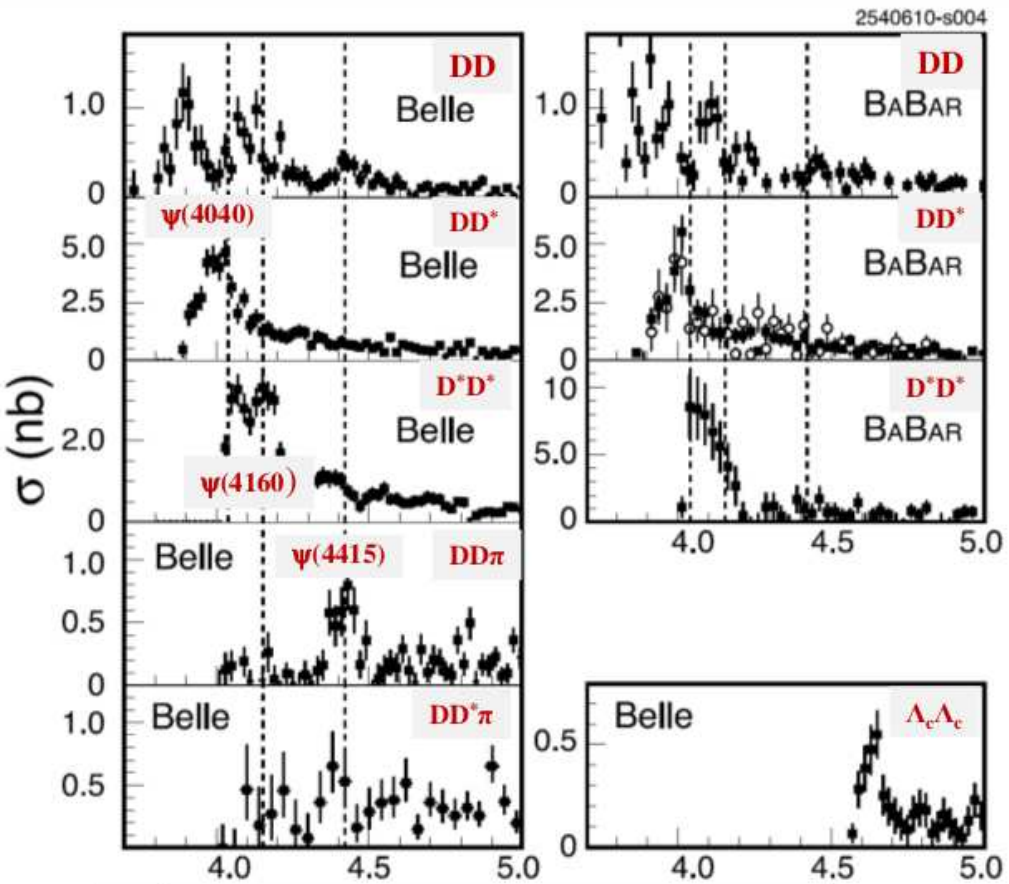

- Belle and BaBar results agree with each other *(see last slide for references)*
- Statistics is too low to study the structure of the cross sections
- Sum of all measured excusive cross-section to open-charm channels saturates the total cross section

Comparison with previous results

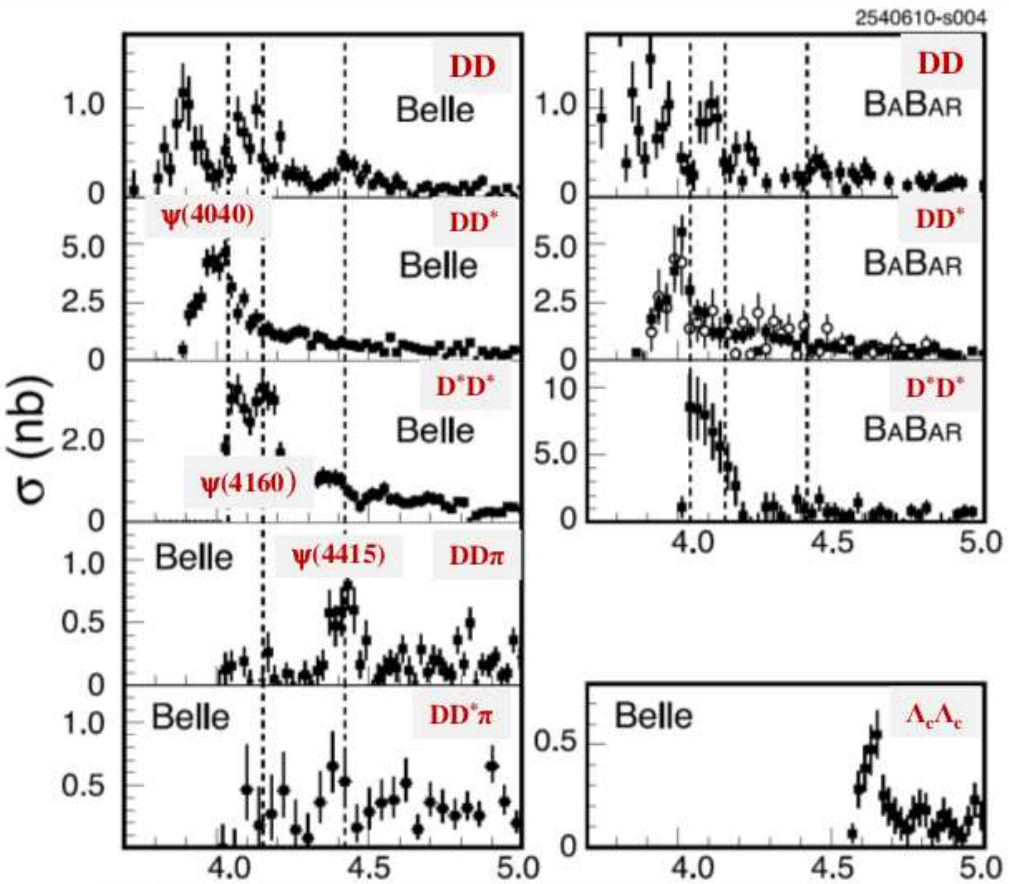

- Belle and BaBar results agree with each other *(see last slide for references)*
- Statistics is too low to study the structure of the cross sections
- Sum of all measured excusive cross-section to open-charm channels saturates the total cross section

Goals:

- To improve accuracy of cross section measurements
- To measure separately cross sections for all 3 possible helicity combinations (TT, LT, LL) for the $D^*\bar{D}^*$ final state

Method

- Partial reconstruction
- Reconstruct D^*, γ_{ISR}

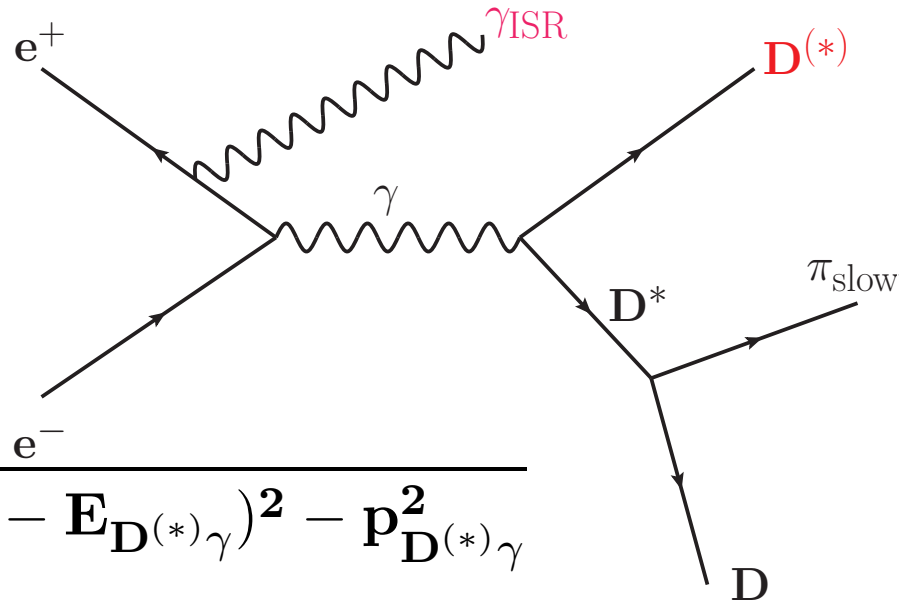

$$M_{recoil}(D^{(*)}\gamma) = \sqrt{(E_{c.m.} - E_{D^{(*)}\gamma})^2 - p^2_{D^{(*)}\gamma}}$$

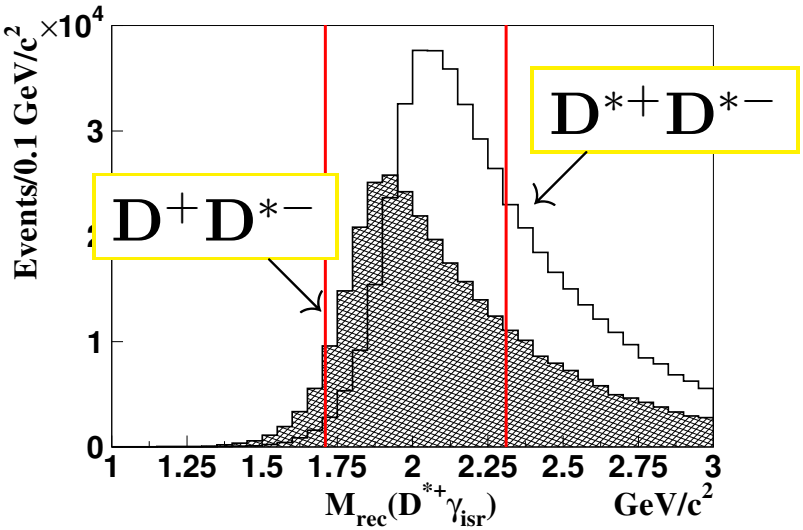

Method

- Partial reconstruction
- Reconstruct $\mathbf{D^*}$, γ_{ISR}

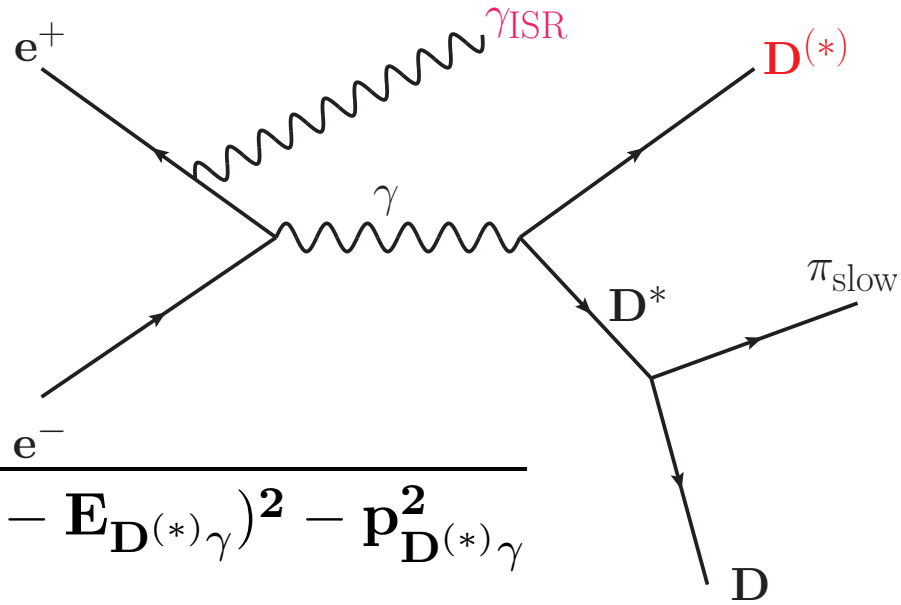

$$M_{recoil}(D^{(*)}\gamma) = \sqrt{(E_{c.m.} - E_{D^{(*)}\gamma})^2 - p^2_{D^{(*)}\gamma}}$$

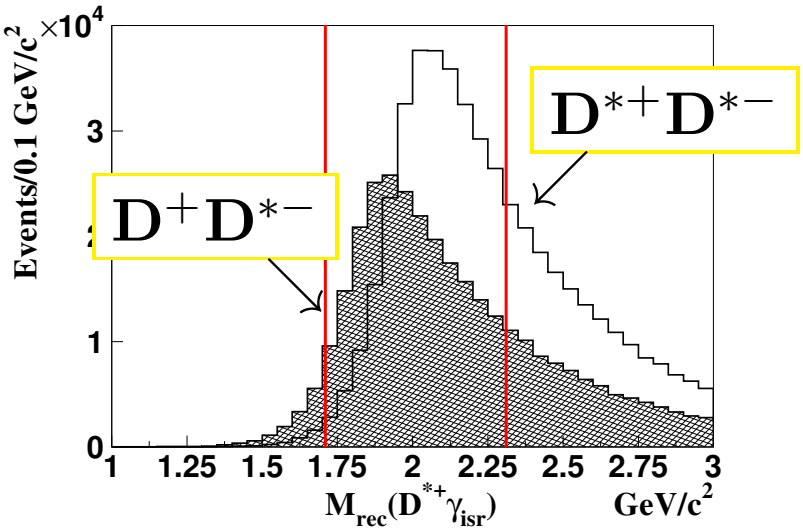

Problem: Cannot distinguish between $\mathbf{D}$, $\mathbf{D^*}$ and $\mathbf{D^{**}}$ in the final state

Method

- Partial reconstruction
- Reconstruct $\mathbf{D}^*$, γ_{ISR} and $\pi_{\mathbf{slow}}$

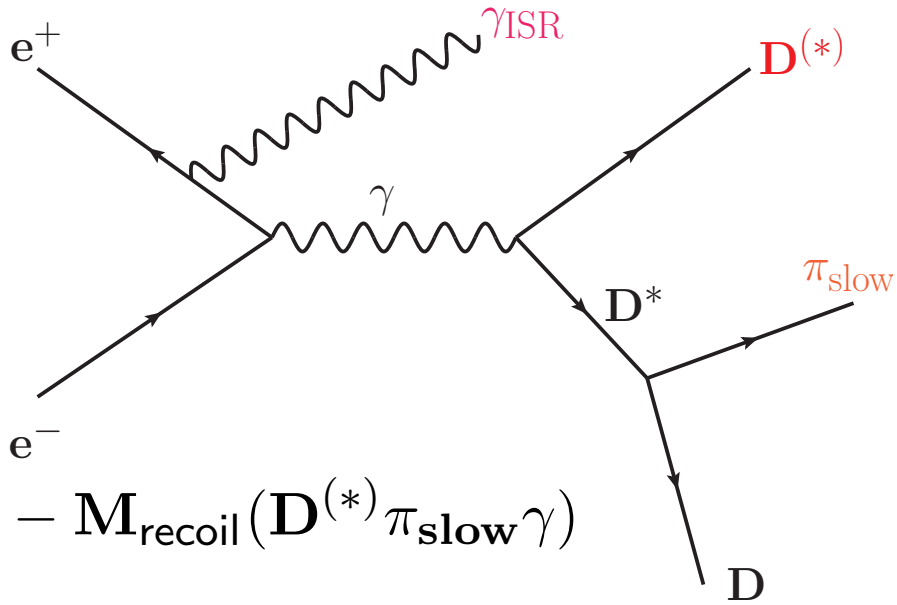

$$\Delta \mathbf{M}_{\mathrm{recoil}} = \mathbf{M}_{\mathrm{recoil}}(\mathbf{D}^{(*)}\gamma_{\mathrm{ISR}}) - \mathbf{M}_{\mathrm{recoil}}(\mathbf{D}^{(*)}\pi_{\mathbf{slow}}\gamma)$$

$\mathbf{e^+e^-} \rightarrow \mathbf{D^+D^{*-}}$

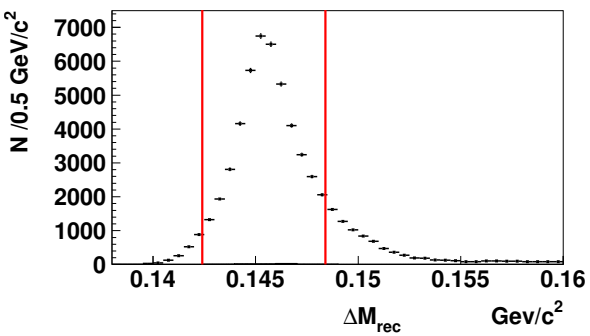

Recoil mass difference $\Delta \mathbf{M}_{\mathrm{recoil}}$

cut:

$\pm 3 MeV/c^2$

$\mathbf{e^+e^-} \rightarrow \mathbf{D^{*+}D^{*-}}$

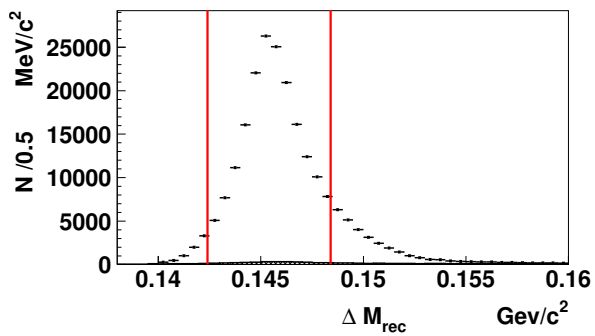

Method

- Partial reconstruction
- Reconstruct $\mathbf{D^*}$, γ_{ISR} and $\pi_{\mathbf{slow}}$
- $\mathbf{M(D^{(*)+}D^{*-}) \equiv M_{recoil}(\gamma_{ISR})}$

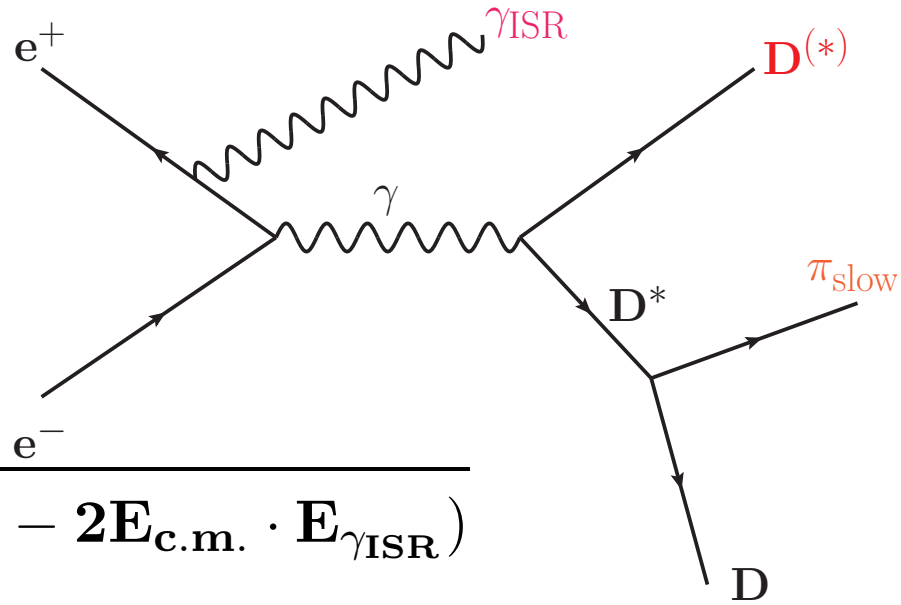

$$\mathbf{M_{recoil}(\gamma_{ISR}) = \sqrt{(E^2_{c.m.} - 2E_{c.m.} \cdot E_{\gamma_{ISR}})}}$$

Refit $M_{\mathrm{recoil}}(D^{(*)}\gamma_{\mathrm{ISR}})$ to D^* mass to improve the $M_{\mathrm{recoil}}(\gamma_{\mathrm{ISR}})$ resolution

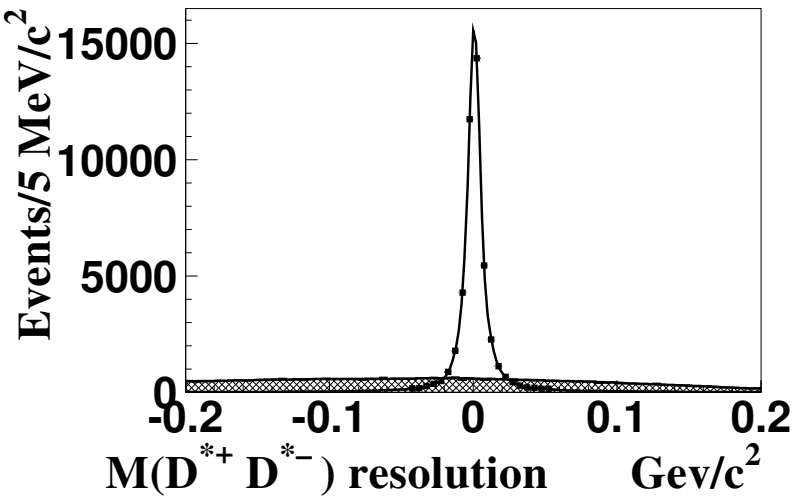

$\mathbf{M_{recoil}(\gamma_{ISR})}$ resolution:

Before re-fit — hatched histogram
After re-fit — solid line

Comparison with previous analysis

- Increased data sample: 547 fb^{-1} $\Longrightarrow$ 951 fb^{-1}
- Additional modes for D reconstruction $\Longrightarrow$ $\mathbf{D^0}$ decay channels:
- Extended signal region for $M_{\text{recoil}}(D^{(*)}\gamma_{\text{ISR}})$

$$|(M_{\text{recoil}}(D^{(*)+}\gamma_{\text{ISR}}) - M(D^{*-}))| < \cancel{200}\ 300\ \text{MeV}/c^2$$

- $\sigma[e^+e^- \to D^{(*)+}D^{*-}] = \dfrac{dN/dM}{\eta_{\text{tot}}(M) \cdot dL/dM}$

dL/dM up to second-order QED corrections

(Kuraev & Fadin (1985))

1. $K^-\pi^+$
2. K^-K^+
3. $K^-\pi^-\pi^+\pi^+$
4. $K^0_S\pi^+\pi^-$
5. $K^-\pi^+\pi^0$
6. $K^0_SK^+K^-$
7. $K^0_S\pi^0$
8. $K^-K^+\pi^-\pi^+$
9. $K^0_S\pi^+\pi^-\pi^0$

Backgrounds

1. Combinatorial background under the reconstructed $D^{(*)+}$ peak
2. Real $D^{(*)+}$ mesons and a combinatorial π_{slow}
3. Both the $D^{(*)+}$ meson and π_{slow} are combinatorial
4. Reflections from the processes $e^+e^- \to D^{(*)+}D^{*-}\pi^0\gamma_{\text{ISR}}$ where the π^0 is lost
5. Contribution of the $e^+e^- \to D^{(*)+}D^{*-}\pi^0_{\text{fast}}$ where the hard π^0_{fast} is misidentified as γ_{ISR}

Background contribution estimated from the data

Mass spectra

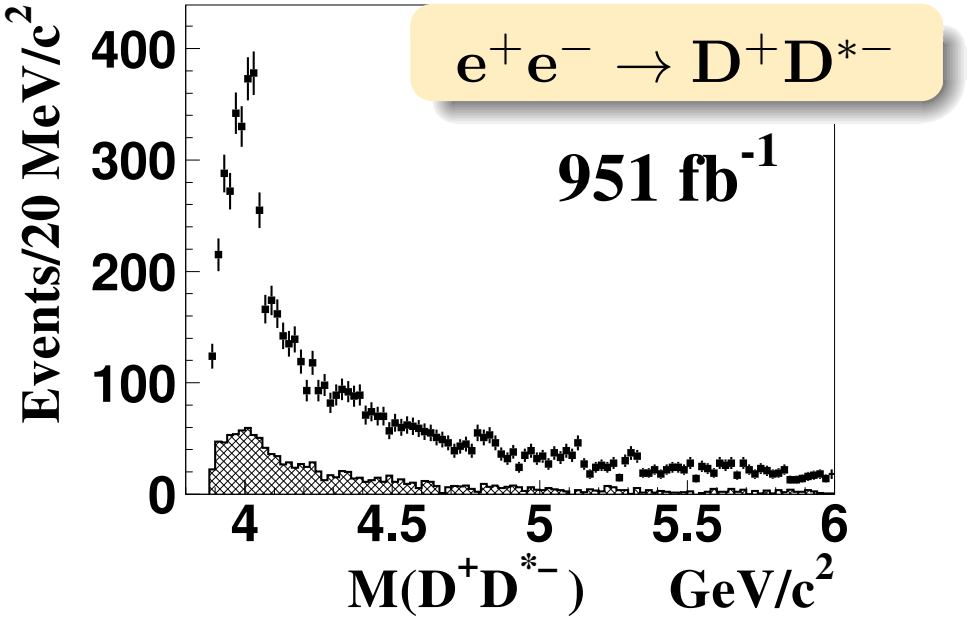

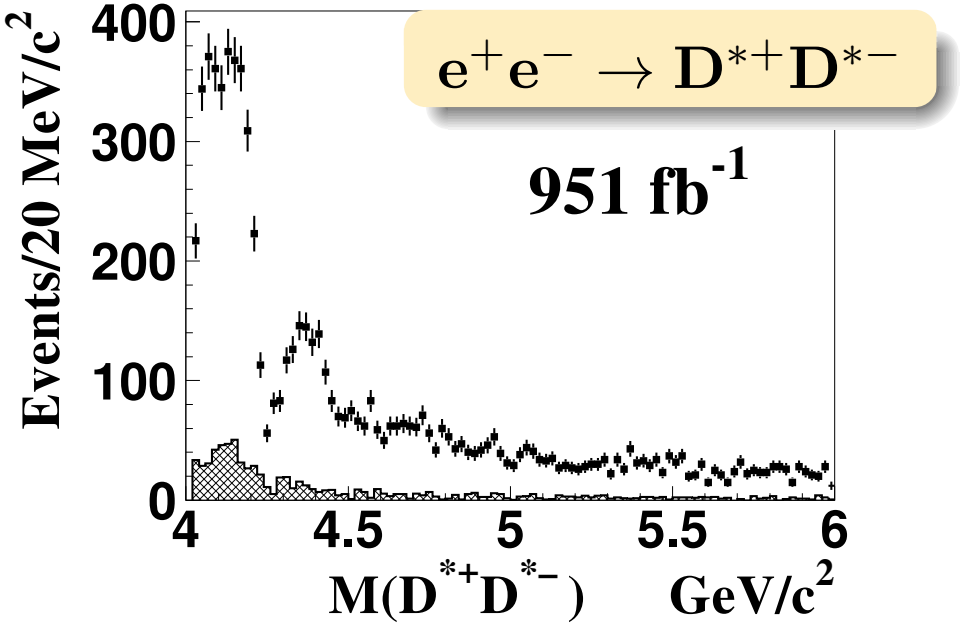

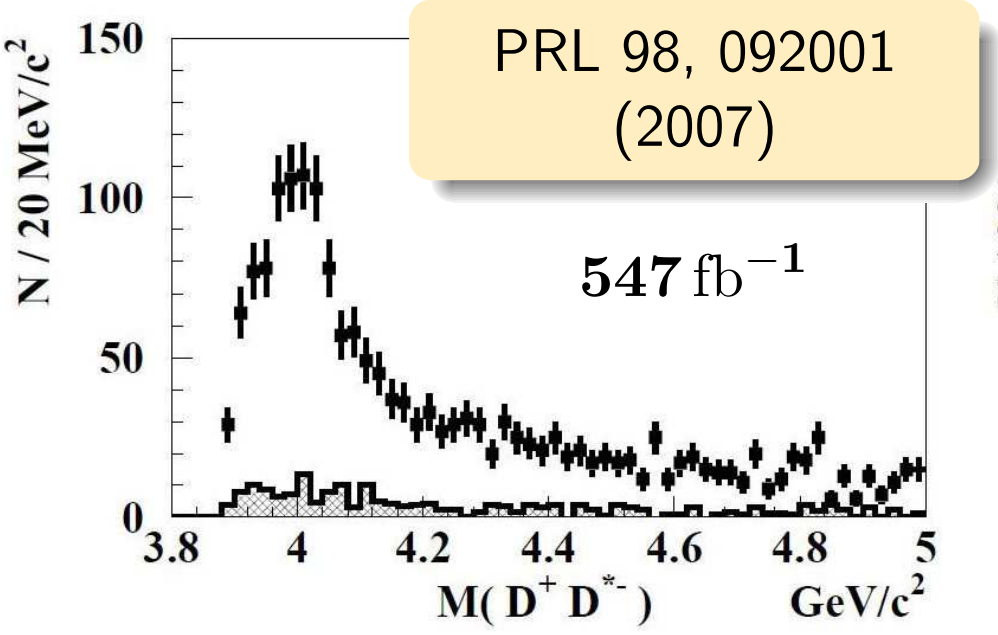

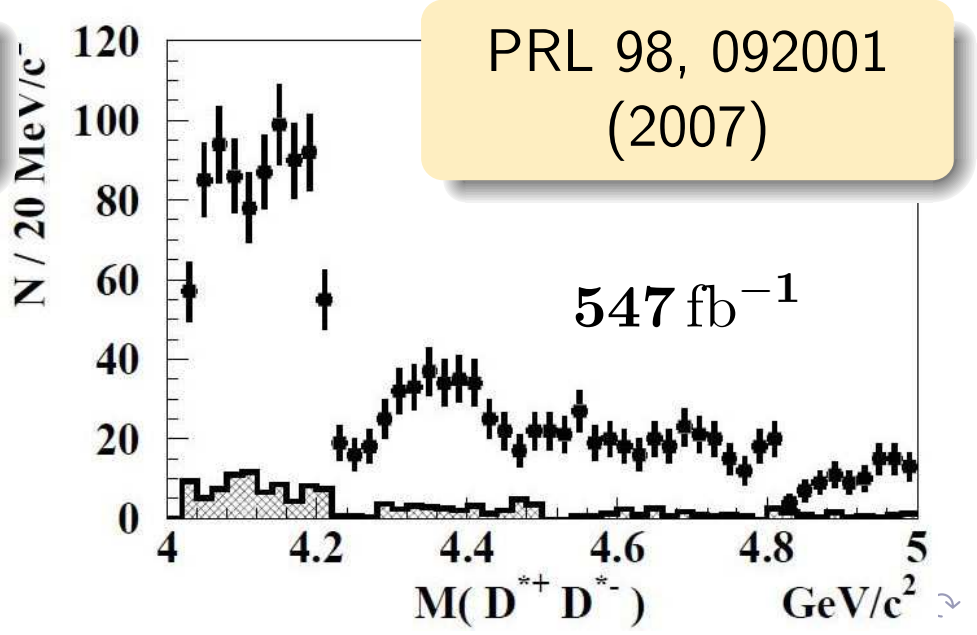

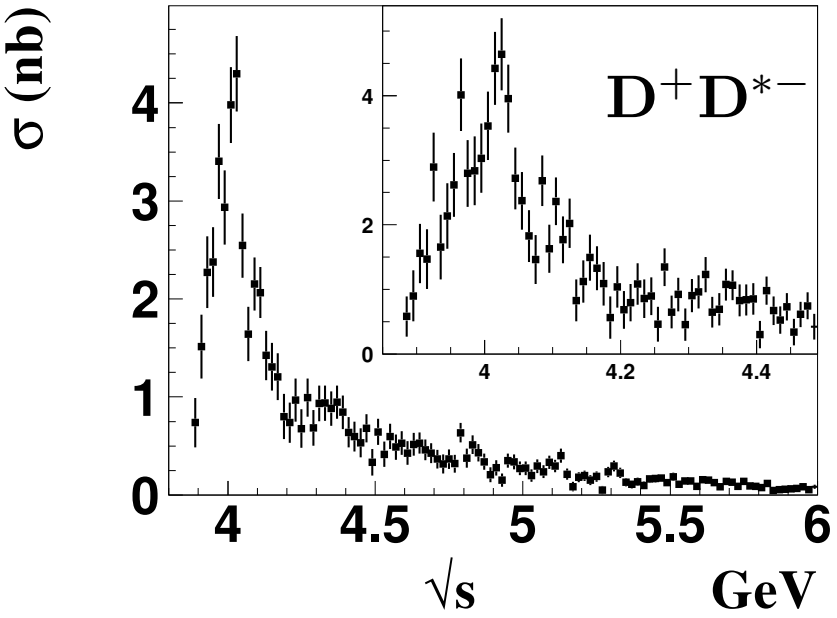

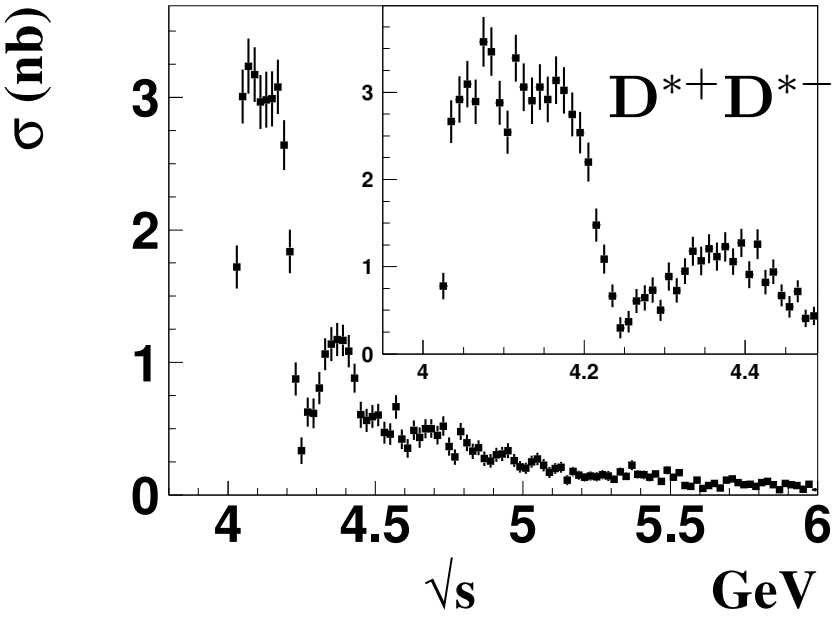

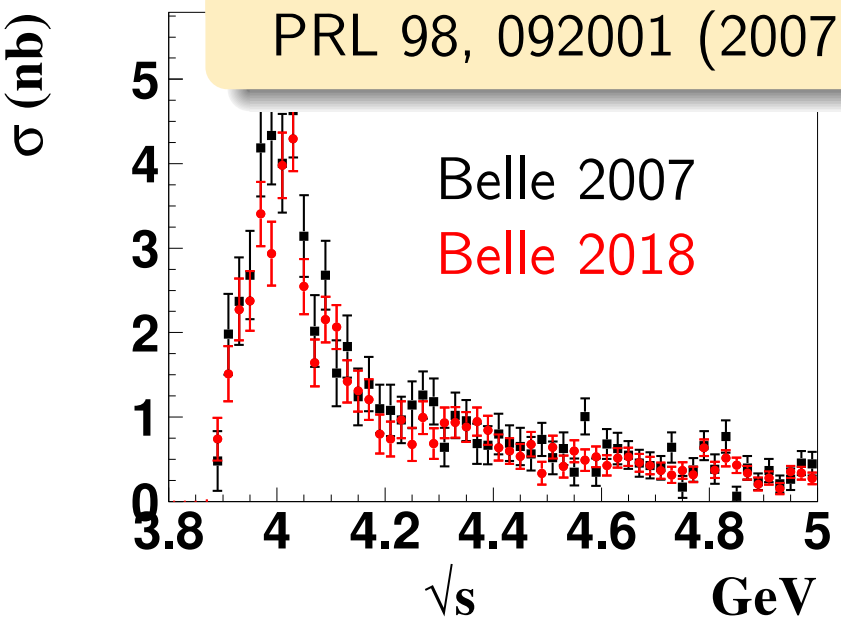

PRL 98, 092001 (2007)

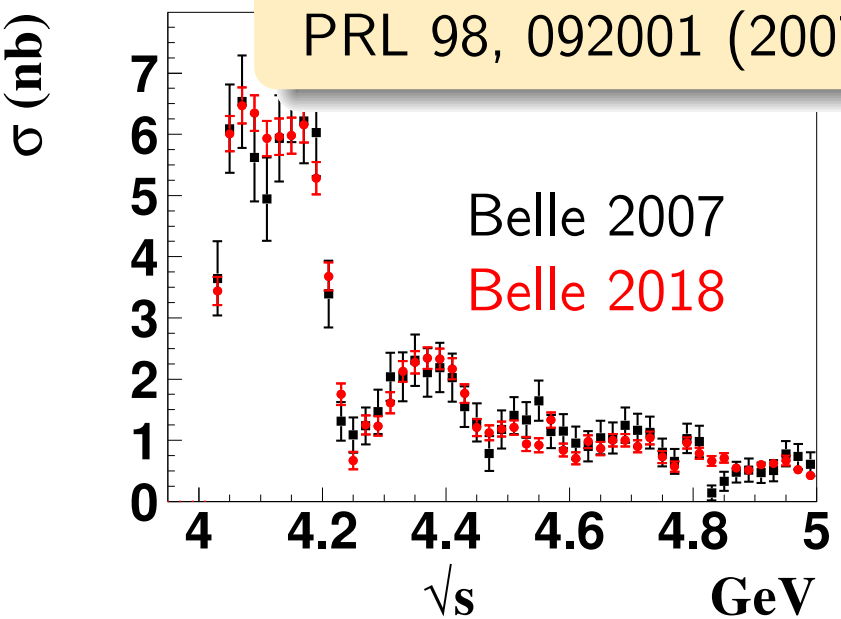

PRL 98, 092001 (2007)

Angular analysis of the process $e^+e^- \to D^+D^{*-}$

- Study D^* helicity angle distribution in each bin of $M(D^+D^{*-})$
- D^* are transversely polarized
  $\Longrightarrow$ Check method

$$4.05 < M(D^+D^{*-}) < 4.3\mathrm{GeV}/c^2$$

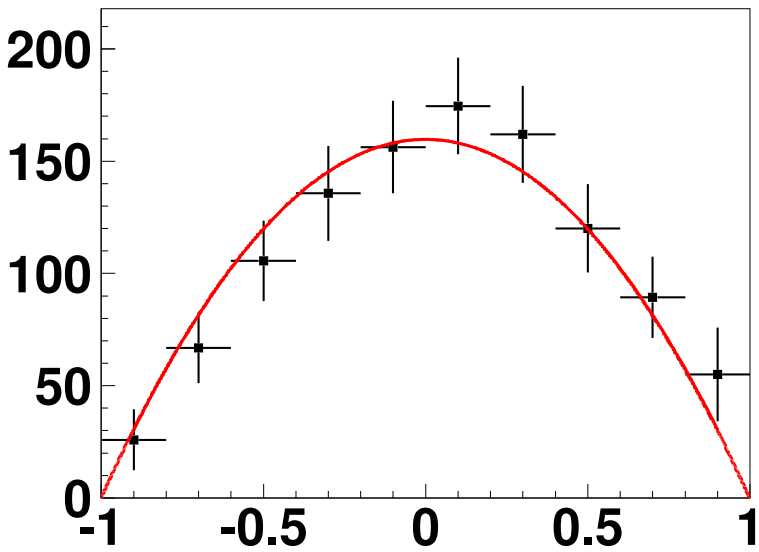

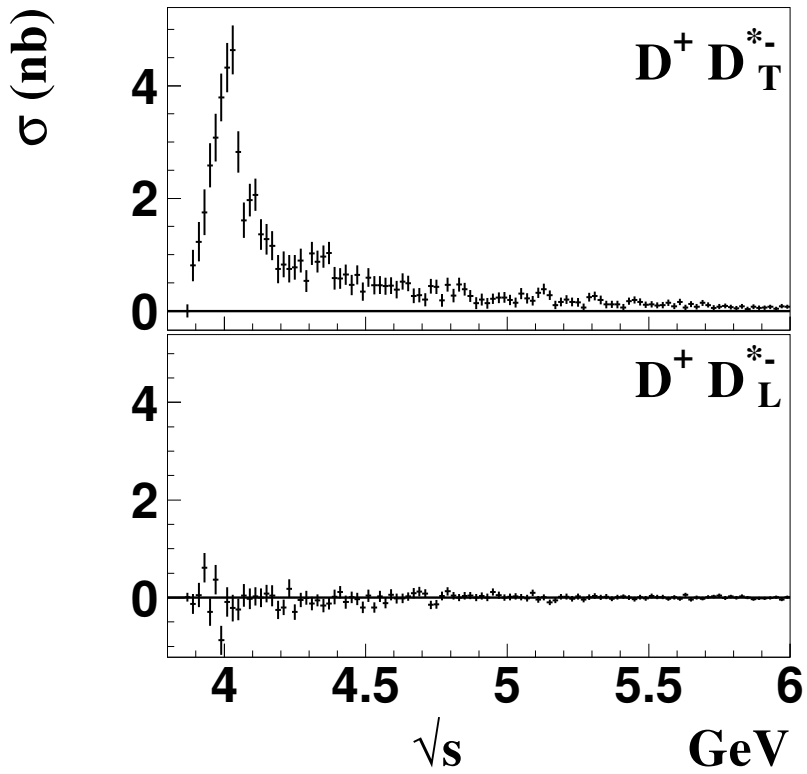

$$f_L = \sigma_L \cdot \cos^2\theta$$
$$f_T = \sigma_T \cdot (1 - \cos^2\theta)$$

$$F(\cos\theta) = \eta(\cos\theta) \cdot dM/dL \cdot (f_L + f_T)$$

Angular analysis of the process $e^+e^- \to D^{*+}D^{*-}$

- Study of the D^* helicity angle distribution in each bin of $M(D^{*+}D^{*-})$
- Helicity composition of the $D^{*+}D^{*-}$ final state:

$$\mathbf{D}^{*+}_{\mathrm{T}}\mathbf{D}^{*-}_{\mathrm{T}},\ \mathbf{D}^{*+}_{\mathrm{T}}\mathbf{D}^{*-}_{\mathrm{L}} \text{ and } \mathbf{D}^{*+}_{\mathrm{L}}\mathbf{D}^{*-}_{\mathrm{L}}$$

  - $D^*_{\mathrm{T}} \equiv$ transversely polarized D^* meson
  - $D^*_{\mathrm{L}} \equiv$ longitudinally polarized D^* meson
- Total cross section

$$\sigma = \sigma_{\mathrm{TT}} + \sigma_{\mathrm{TL}} + \sigma_{\mathrm{LL}}$$

$$f = \eta(c_1, c_2) \cdot dL/dM \cdot (f_{LL} + f_{TL} + f_{TT}) + f_{\mathrm{bg}}$$

$c_1 \equiv \cos\theta_f \qquad c_2 \equiv \cos\theta_p$

θ's are D^*'s helicity angles

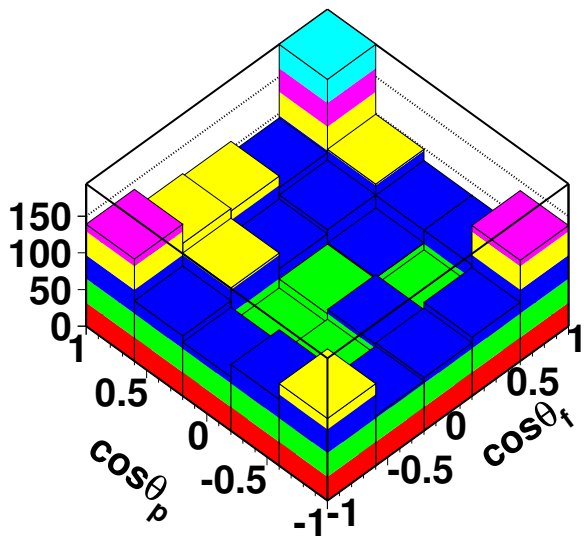

$$\begin{aligned} f_{TT} &= \sigma_{TT} \cdot (1 - c_1^2) \cdot (1 - c_2^2) \\ f_{TL} &= \sigma_{TL} \cdot \left((1 - c_1^2) \cdot c_2^2 + c_1^2 \cdot (1 - c_2^2)\right) \\ f_{LL} &= \sigma_{LL} \cdot c_1^2 \cdot c_2^2 \end{aligned}$$

Fit results

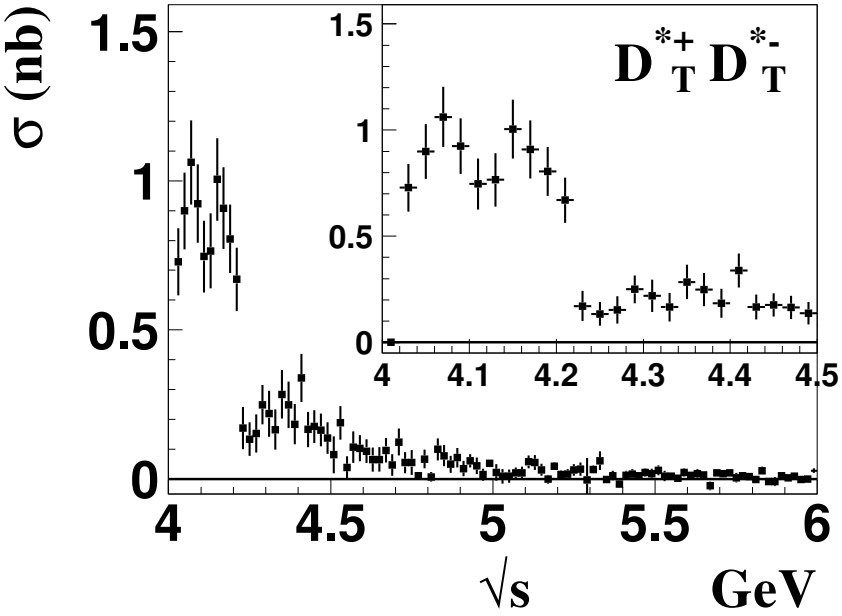

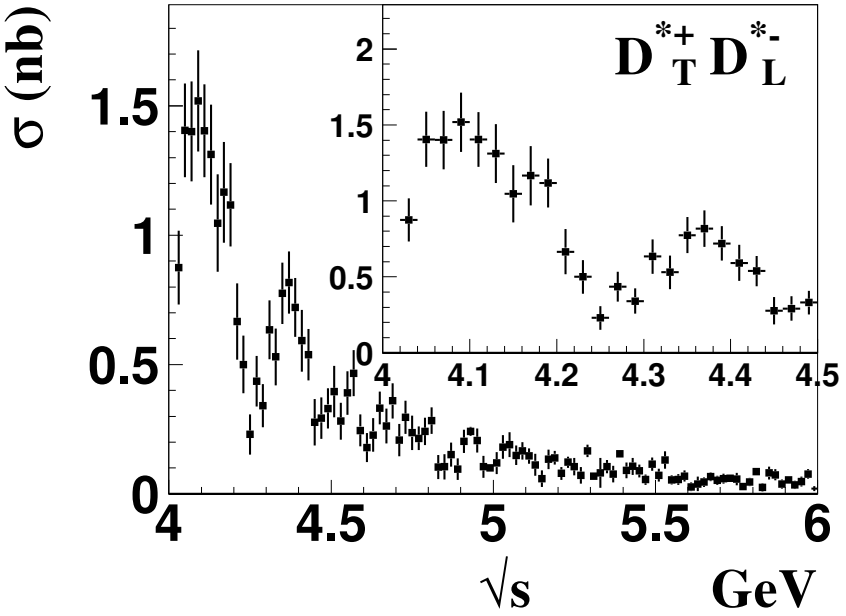

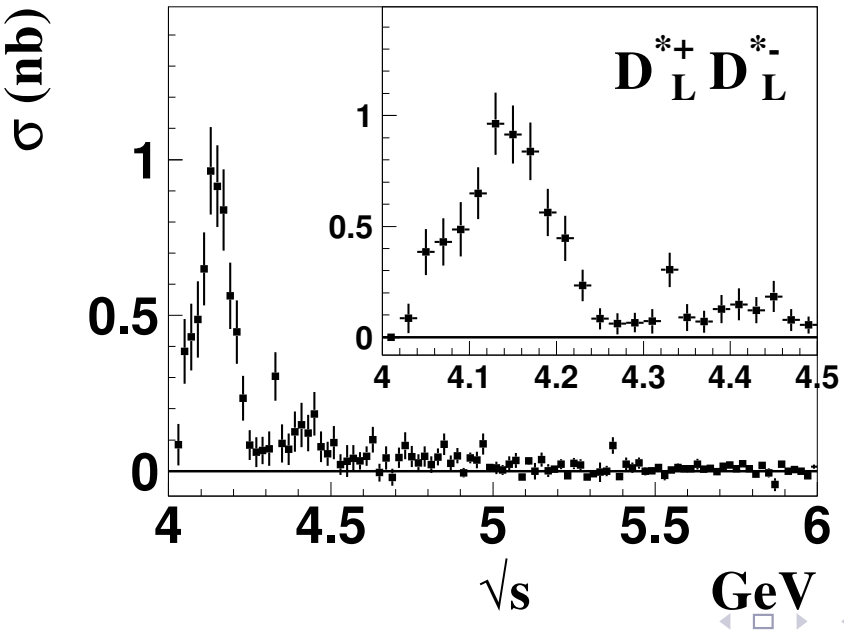

Conclusions

- We measured the exclusive cross sections of the $e^+e^- \to D^+D^{*-}$ and $e^+e^- \to D^{*+}D^{*-}$ processes
- The accuracy of the cross section measurements is increased
- The systematic uncertainties are significantly reduced
- For the $e^+e^- \to D^{*+}D^{*-}$ process we measured separately the cross sections for all three possible helicity final states (TT, LT and LL)

Conclusions

- We measured the exclusive cross sections of the $e^+e^- \to D^+D^{*-}$ and $e^+e^- \to D^{*+}D^{*-}$ processes
- The accuracy of the cross section measurements is increased
- The systematic uncertainties are significantly reduced
- For the $e^+e^- \to D^{*+}D^{*-}$ process we measured separately the cross sections for all three possible helicity final states (TT, LT and LL)

Thank you for your attention!

References

1. Phys. Rev. D**77**,011103 (2008)
2. Phys. Rev. Lett.**98**, 092001 (2007)
3. Phys. Rev. Lett.**100**, 062001 (2007)
4. Phys. Rev. Lett.**101**, 172001 (2008)
5. Phys. Rev. D**80**, 091101(R) (2009)
6. Phys. Rev. D**76**, 111105(R) (2007)
7. Phys. Rev. D**79**, 092001 (2009)

Initial state radiation

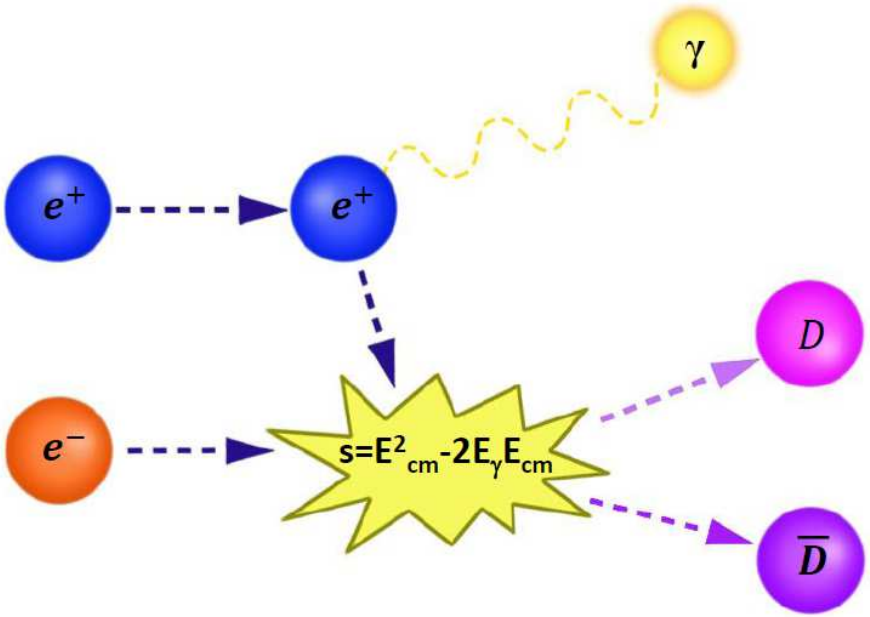

1. Allows to study energies below $E_{\mathrm{c.m.}}$
2. Wide energy range available for the cross section measurements
3. Suppression from additional photon emission compensated by high luminosity at B-factory

We use the data sample collected with the Belle detector with the integrated luminosity of 951 fb^{-1}

Reflection from the processes $e^+e^- \to D^{(*)+}D^{*-}\pi^0\gamma_{ISR}$

$e^+e^- \to D^+D^{*-}$

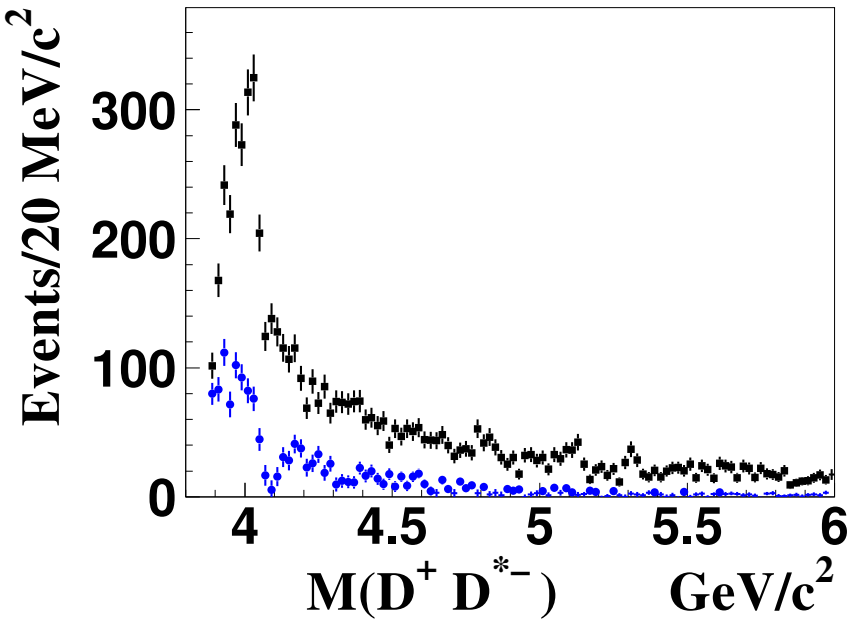

$e^+e^- \to D^{*+}D^{*-}$

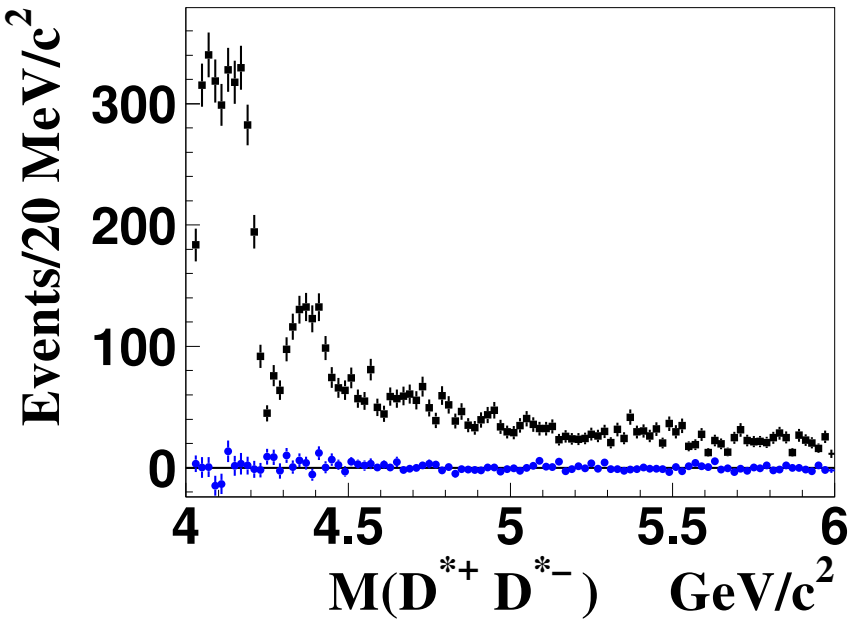

Background (blue points) from

$$e^+e^- \to D^{(*)+}D^{*-}\pi^0_{\text{miss}}\gamma_{\text{ISR}}$$

is evaluated from the isospin-conjugated process

$$e^+e^- \to D^{(*)0}D^{*-}\pi^+_{\text{miss}}\gamma_{\text{ISR}}$$

with the reconstruction of $D^{(*)0}$, π^-_{slow} and γ_{ISR}

Criteria

- $|dr| < 2\,\mathrm{cm}$ and $|dz| < 4\,\mathrm{cm}$
- $\mathcal{P}_{K/\pi} = \mathcal{L}_K/(\mathcal{L}_K + \mathcal{L}_\pi) > 0.6$

K_S candidates:

- $|M_{inv}(\pi^+\pi^-) - M_{K^0_S}| < 15$ MeV/c^2
- the distance between the two pion tracks $< 1\,\mathrm{cm}$
- the transverse flight distance from IP $> 0.1\,\mathrm{cm}$
- the angle between the K_S momentum direction and decay path in $x-y$ plane $< 0.1\,\mathrm{rad}$

π_0 candidates:

- $|M_{inv}(\gamma\gamma) - M_{\pi_0}| < 15$ MeV/c^2

D^0 decay channels:

1. $K^-\pi^+$
2. K^-K^+
3. $K^-\pi^-\pi^+\pi^+$
4. $K^0_S\pi^+\pi^-$
5. $K^-\pi^+\pi^0$
6. $K^0_SK^+K^-$
7. $K^0_S\pi^0$
8. $K^-K^+\pi^-\pi^+$
9. $K^0_S\pi^+\pi^-\pi^0$

D^+ decay channels:

1. $K^+\pi^-\pi^-$
2. $K^0_S\pi^-$
3. $K^0_SK^+$

D^* decay channels:

1. $D^0\pi^+$

Analysis of the process $e^+e^- \to D^{(*)+}D^{*-}$

Method:

- partial reconstruction;
- reconstruction D^*, π_{slow} and γ_{ISR};

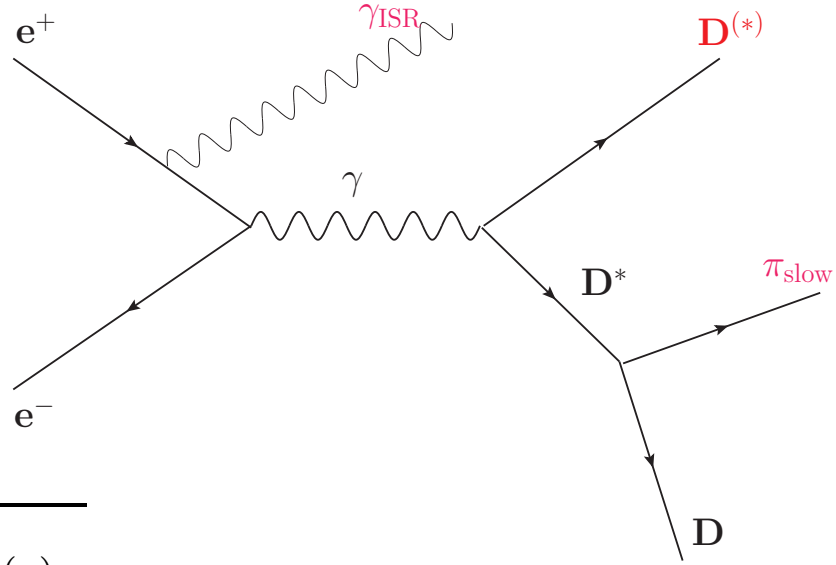

$$M_{recoil}(D^{(*)}\gamma) = \sqrt{(E_{c.m.} - E_{D^{(*)}\gamma})^2 - p^2_{D^{(*)}\gamma}}$$

$$\Delta M_{recoil} = M_{recoil}(D^{(*)}\gamma_{ISR}) - M_{recoil}(D^{(*)}\pi_{slow}\gamma)$$

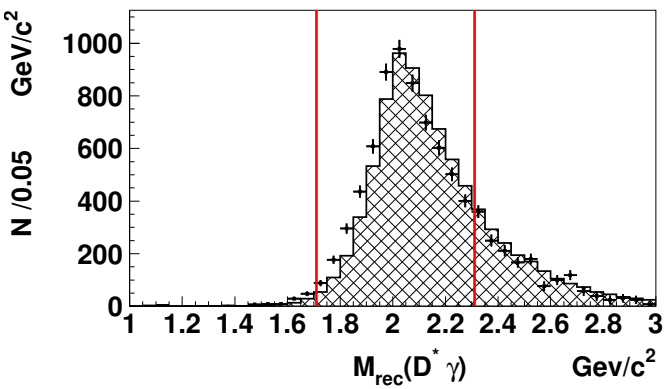

Spectrum of $M_{recoil}(D^*\gamma_{ISR})$

$$M_{recoil}(D^{(*)}\gamma) = \sqrt{(E_{c.m.} - E_{D^{(*)}\gamma})^2 - p^2_{D^{(*)}\gamma}}$$

Correction of γ_{ISR} energy

reference channel

$$e^+e^- \to \psi(2S)\gamma_{ISR}$$
$$\searrow$$
$$\psi(2S) \to J/\psi\pi^+\pi^-$$

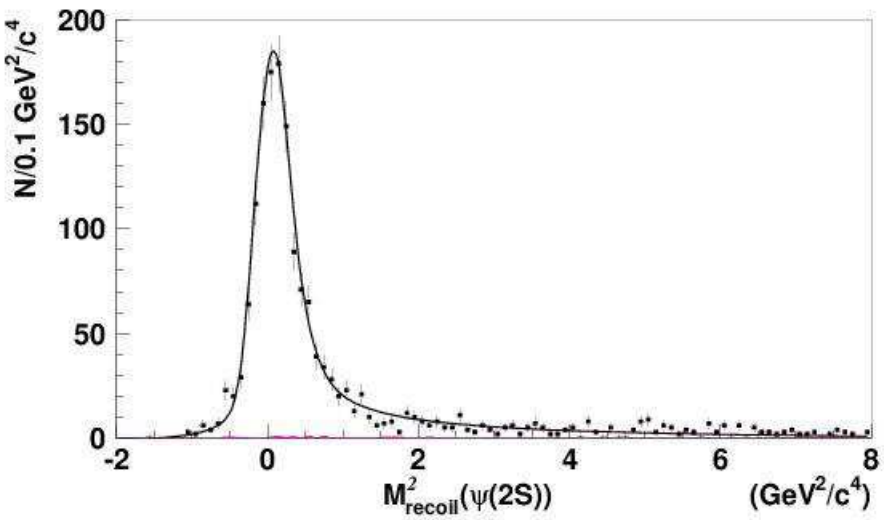

The same process on the other side

The recoil mass $\mathbf{M_{recoil}(J/\psi\pi^+\pi^-)}$

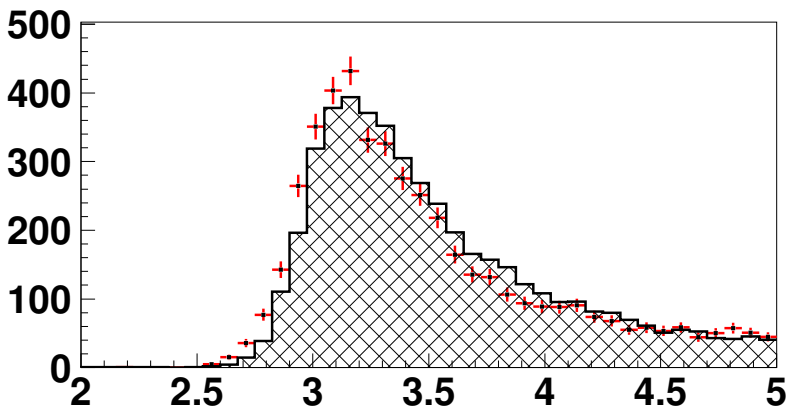

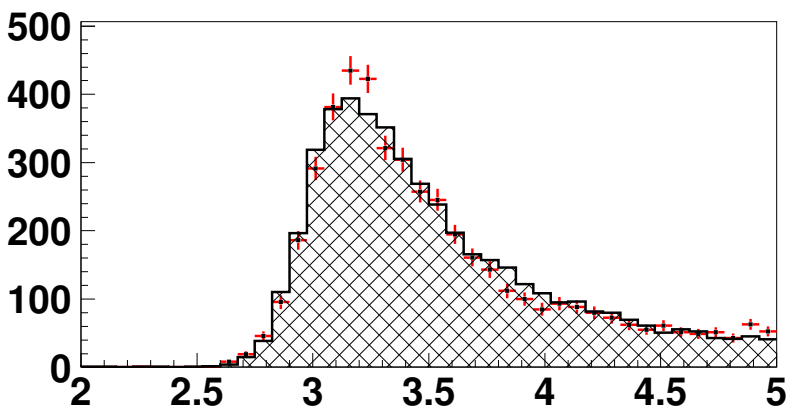

Conclusions:

phokhara generator describes the second radiation correction correctly

The recoil mass $M_{\text{recoil}}(D^*\gamma_{\text{ISR}})$

before correction γ_{ISR} energy

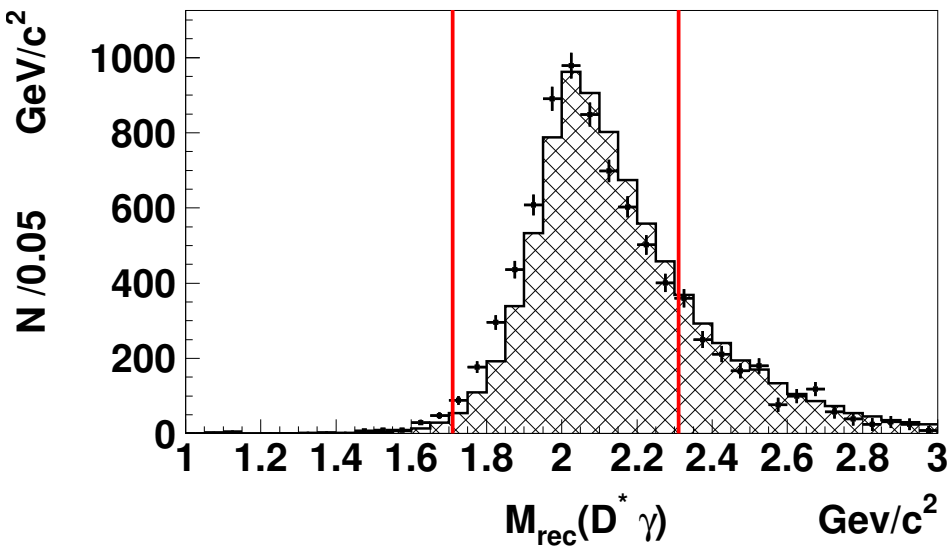

after correction γ_{ISR} energy

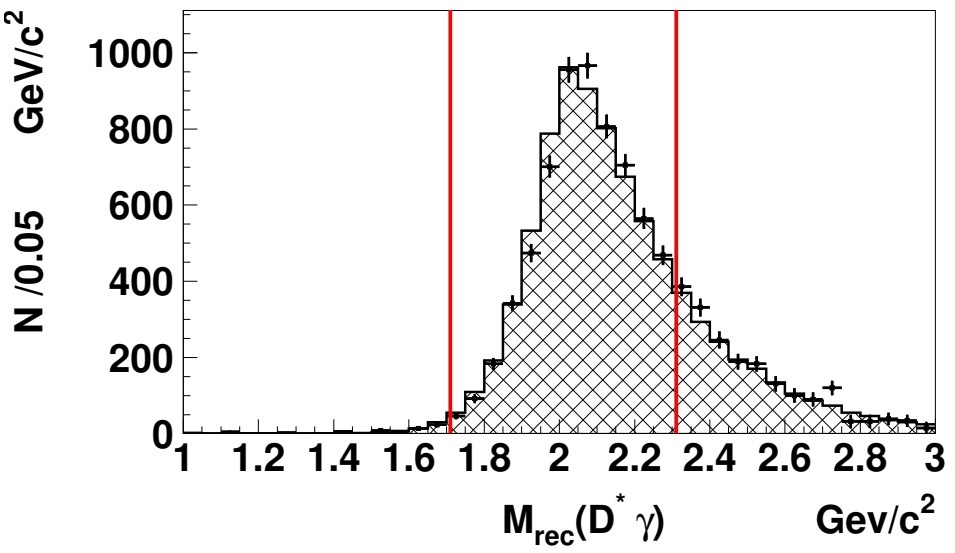

cut:

$$|M_{\text{recoil}}(D^*\gamma_{\text{ISR}}) - M(D^*)| < 300 MeV/c^2$$

Backgrounds

1. Combinatorial background under the reconstructed $D^{(*)+}$ peak
2. Real $D^{(*)+}$ mesons and a combinatorial π_{slow}
3. Both the $D^{(*)+}$ meson and π_{slow} are combinatorial
4. Reflections from the processes $e^+e^- \to D^{(*)+}D^{*-}\pi^0\gamma_{\text{ISR}}$ where the π^0 is lost
5. Contribution of the $e^+e^- \to D^{(*)+}D^{*-}\pi^0_{\text{fast}}$ where the hard π^0_{fast} is misidentified as γ_{ISR}

$\mathbf{e^+e^- \to D^+D^{*-}}$

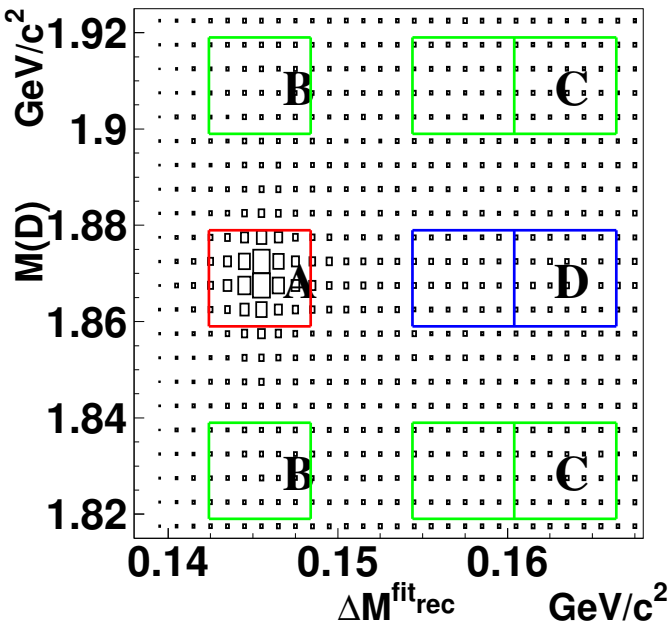

$\mathbf{e^+e^- \to D^{*+}D^{*-}}$

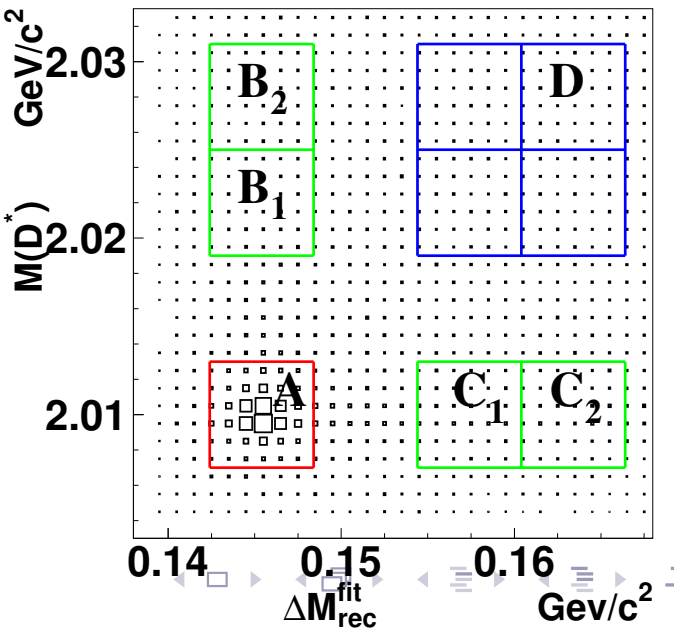

Cross sections calculation

$e^+e^- \to D^+D^{*-}$

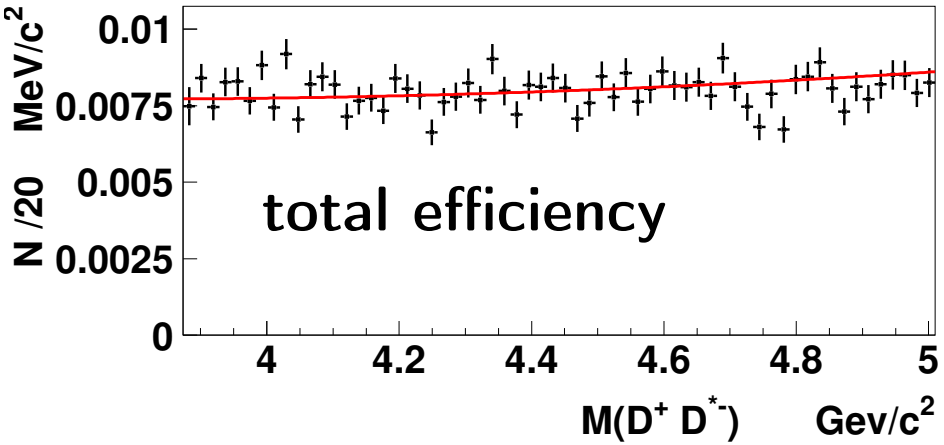

$$\sigma_{e^+e^- \to D^{(*)}+D^{*-}} = \frac{dN/dM}{\eta_{tot}(M) \cdot dL/dM}$$

$e^+e^- \to D^{*+}D^{*-}$

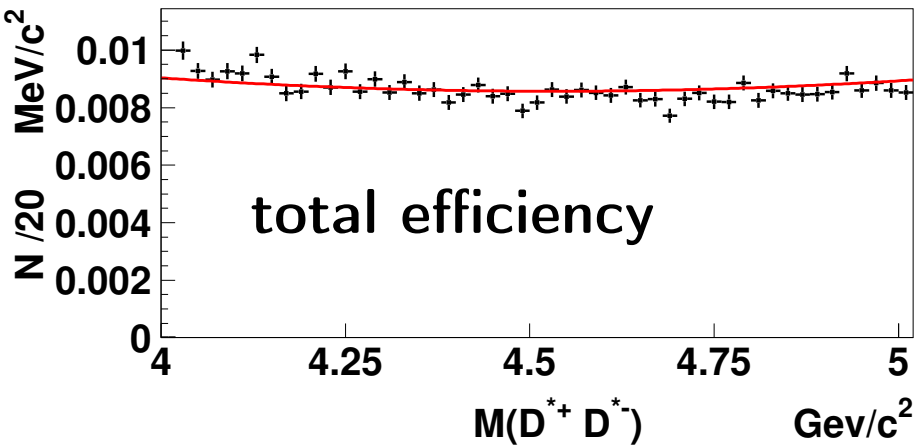

dN/dM - mass spectrum,

η_{tot} - total efficiency,

dL/dM - differential luminosity;

$4.0 < M(D^{*+}D^{*-}) < 4.1\mathrm{GeV}/c^2$

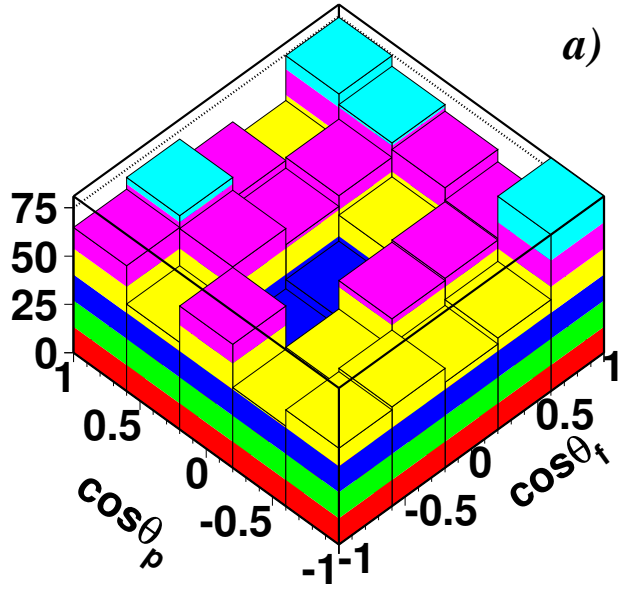

$4.1 < M(D^{*+}D^{*-}) < 4.25\mathrm{GeV}/c^2$

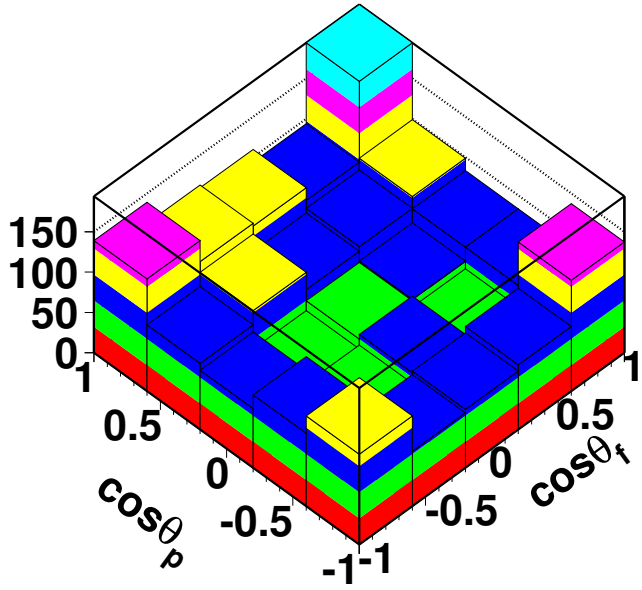

$4.25 < M(D^{*+}D^{*-}) < 4.6\mathrm{GeV}/c^2$

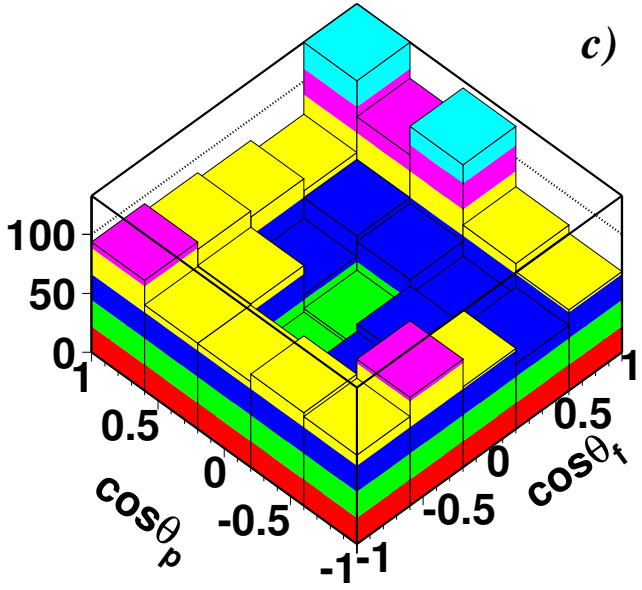

$M(D^{*+}D^{*-}) > 4.6\mathrm{GeV}/c^2$

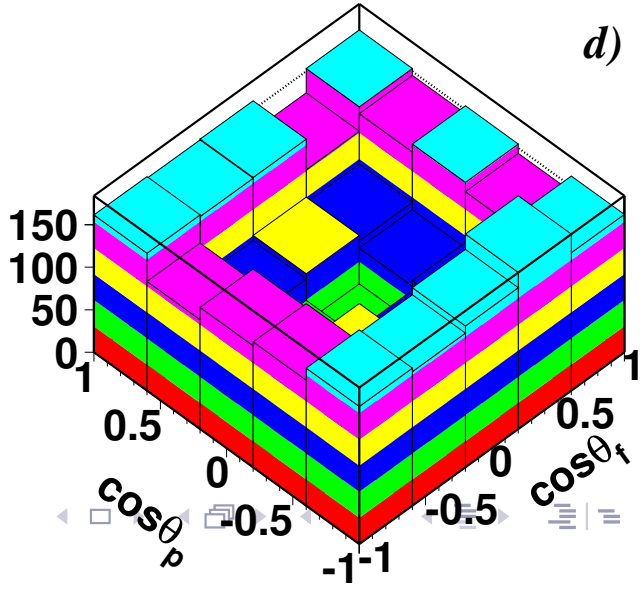

The summary of the systematic errors in the cross section calculation.

Source	D^+D^{*-}	$D^{*+}D^{*-}$
Background subtraction	2%	2%
Reconstruction	3%	4%
Selection	1%	1%
Angular distribution	–	2%
Cross section calculation	1.5%	1.5%
$\mathcal{B}(D^{(*)})$	2%	3%
MC statistics	1%	2%
Total	5%	7%